

Final Report: A Comparative Study of Heat Distribution and Cost Effectiveness of Cooking Pans

Group Members: Lokesh Sriram, Yuchen Fu, Owen Campbell, Kailash Senthilkumar

Lab Div: ME31500-050

Date: 11/20/24

TA: Justin Ramey

Table of Contents

Executive Summary	3
Experimental Method	5
Analysis	8
Results and Discussion.....	11
Conclusions	17
References	19
Appendix:.....	20
I.Property Tables:	20
II.Sample Calculations	20

Executive Summary

This research investigated the thermal performance characteristics of stainless-steel cookware, focusing on comparing pans with and without a copper core. The primary objective was to comprehensively assess heat distribution uniformity, cost-efficiency, and thermal transfer mechanisms across different pan configurations. The study employed a centrally mounted patch heater, high-resolution infrared thermal imaging, and advanced analytical modeling to systematically evaluate the thermal behavior of two 10-inch stainless steel pans. Key findings revealed the thermal performance for the copper core pan to be superior. The copper core pan showcased 29% enhancement in heat distribution uniformity, with the standard deviation reduced from 3.2815 to 1.7603. Furthermore, it demonstrated an 86.8% reduction in temperature variability per dollar, with Temperature Cost Ratio (TCR) of 0.09 K/\$ in comparison to the 0.68 K/\$. These results indicated significantly more consistent and predictable heating characteristics, with analytical modeling showing substantially lower percentage errors compared to the non-core pan. The practical implications of this research extend beyond academic interest, offering valuable insights for both manufacturers and consumers. The study provides a quantitative assessment of how core designs can optimize thermal performance in cookware. The copper core pans not only demonstrated superior heat distribution but also suggested potential energy efficiency improvements and enhanced cooking outcomes.

Looking forward, further investigation into experimental setups that more closely simulate real-world cooking conditions, exploration of alternative core materials, and comprehensive analyses of dynamic temperature scenarios. The foundational framework established by this study opens new avenues for material innovation in cookware engineering, emphasizing the critical role of thermal management in culinary equipment design. In conclusion, this exploration provides a comprehensive examination of thermal performance in stainless steel cookware, highlighting the significant potential for material-specific improvements. By quantifying the thermal advantages of copper core designs, the study offers a data-driven approach to understanding and optimizing heat transfer mechanisms in cookware, ultimately supporting more efficient and effective cooking technologies.

Introduction

The thermal properties of cookware materials play a crucial role in determining heat distribution across pan surfaces, which directly impacts cooking performance and food quality. Different cookware composites, such as stainless steel and copper, exhibit varying thermal conductivities, leading to significant differences in heat transfer mechanisms during cooking. From a heat transfer perspective, thermal conductivity (k) is a critical material property that governs the rate of heat propagation through solid materials, with copper demonstrating superior conductivity compared to stainless steel (Smith et al., 2020). Understanding these properties is essential for both home cooks and professional chefs, as it enables the selection of appropriate pans for specific culinary tasks, ultimately improving food quality and energy use in kitchens (Johnson & Lee, 2019).

In this project, we aim to investigate the heat distribution characteristics of two types of 10-inch stainless steel pans—one featuring a copper core and the other constructed solely from stainless steel. The primary objectives of this experiment are to compare the temperature profiles of each pan, assess the uniformity of heat distribution, and evaluate the cost efficiency of both cookware types. The experimental methodology involves creating a controlled heating scenario where a patch heater is attached at the bottom center of each pan to provide a uniform heat source. To capture the thermal characteristics, we will use an infrared (IR) camera to obtain thermal images of the pans at steady-state conditions. The IR camera will allow us to capture a comprehensive temperature distribution profile along the radial direction of each pan, enabling a detailed analysis of heat spread from the center to the edges. Our analysis will focus on comparing the temperature gradients between the center and the edges of the pans, providing insights into the thermal distribution of different pan compositions. Additionally, we will evaluate the cost of each pan in relation to its thermal characteristics, offering a comprehensive assessment of the cost-efficiency of different cookware materials. This project will build upon existing literature regarding thermal conductivity and heat transfer in cookware materials, drawing on studies that highlight the importance of material selection in culinary applications (Brown et al., 2021). The results of this experiment will contribute valuable information to both consumers and manufacturers, enhancing understanding of material-specific thermal performance.

Experimental Method

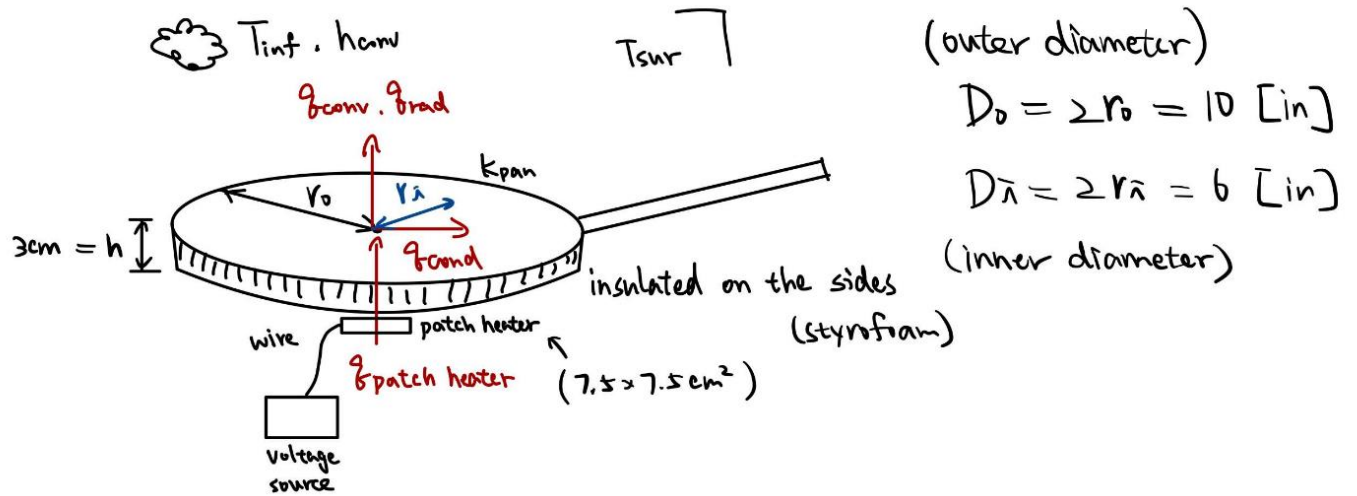


Fig 1. Experimental setup diagram

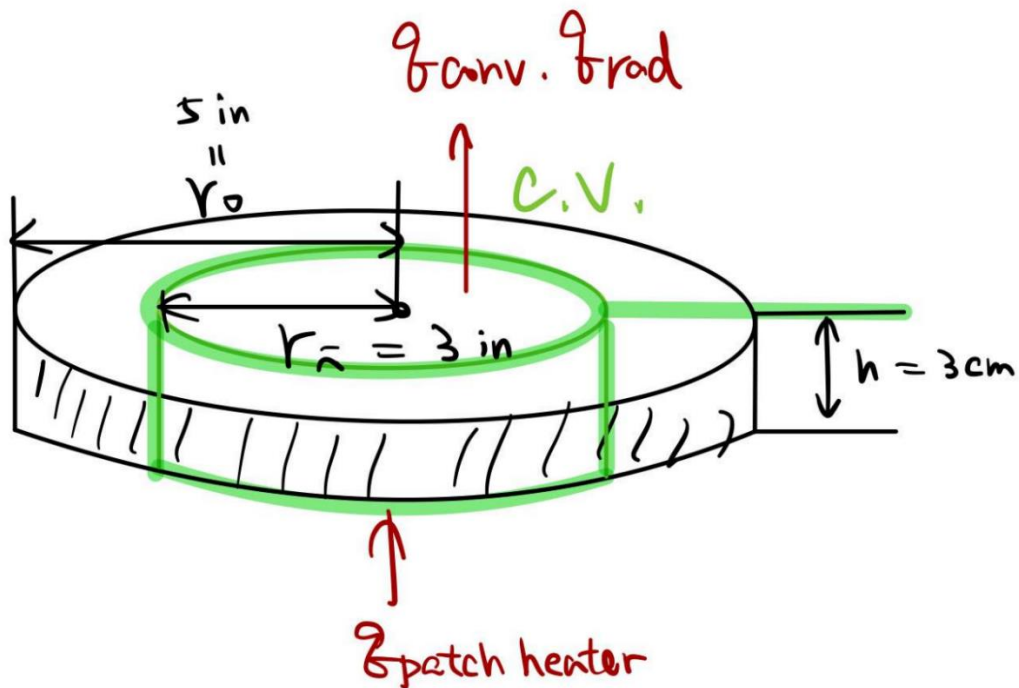


Fig 2. Heat transfer analysis using control volume

The system comprises the following major components:

1. **Copper Core Pan:** A stainless-steel pan with a copper core, which has a 10-inch outer diameter and a 6-in inner diameter
2. **Non-Copper Core Pan:** A stainless-steel pan, which has a 10-inch diameter and a 6-in inner diameter
3. **Patch Heater:** A square heating element (7.5 cm *7.5 cm) placed at the center of the pan.
4. **Insulation:** Styrofoam wrapped around the bottom and sides of the pan to minimize heat loss.
5. **Infrared (IR) Camera:** Positioned 10 inches above the pan to capture infrared thermal data across the surface.

The research investigates heat distribution uniformity across cookware materials through a meticulously designed experimental framework. The primary objective is to comprehensively analyze thermal conductivity variations between stainless steel pans with and without integrated copper cores, providing quantitative insights into heat transfer mechanisms and material performance.

The experimental system comprises two pan variants: a standard stainless-steel pan and a stainless-steel pan with a copper core. Each specimen had a 10-inch outer diameter and a 6-inch inner diameter, ensuring uniformity among the test subjects. A centrally-mounted patch heater served as the uniform heat source. The patch heater was attached to the pan using thermal paste, which ensured optimal heat transfer by reducing contact resistance. To precisely control the power input and monitor its performance, the patch heater was connected to a power meter. This setup allowed us to verify its internal resistance, which was approximately 3.5 W, and to ensure the heater was powered at around 26 W, excluding the internal resistance. (The set of experimental conditions for both the pans can be seen in the Appendix)

Thermal measurements were conducted exclusively using infrared imaging techniques. A high-resolution infrared (IR) camera was used to map the temperatures across the pan's surface. The camera was positioned directly above the pans. Before imaging, the pans were coated with high-emissivity black paint to simulate a black body radiation environment, ensuring uniform and reliable thermal emission measurements.

To minimize heat loss and focus the analysis on radial heat distribution, high-density Styrofoam insulation was applied to the sides and bottoms of the pans. Ambient temperature, which is critical for accurate thermal analysis, was recorded using a digital thermometer to provide reference data.

Thermal imaging was conducted systematically at 4-minute intervals, using SmartView 4.4 software to process the captured images. The system was considered to have reached steady state

when temperature fluctuations at the pan's center remained within 1°C between successive measurements. This approach enabled detailed mapping of the temperature distribution from the center of the pans to their 6-inch inner diameter, providing a comprehensive profile of heat transfer characteristics.

Since the supplier did not provide the thermal conductivity values of the pans, we referred to publicly available data from the Engineering Toolbox website (Engineering Toolbox, n.d) to estimate the thermal conductivities of stainless steel and copper. Note that for the pan with the copper core, the average thermal conductivity between the copper and stainless steel was used. These values were used in our analytical model to calculate heat transfer properties. (The properties used in calculations can be seen in the Appendix)

To ensure the reliability of the experimental procedure, the tests were repeated multiple times. The stainless-steel pan with a copper core was tested twice, while the standard stainless-steel pan without a copper core was tested three times. These repetitions were performed to verify consistency in the results and ensure the experiment was conducted correctly.

The experimental design incorporated rigorous methodological considerations to ensure reproducibility and minimize uncertainties. For instance, the accurate monitoring of the power input, controlled ambient conditions, multiple trials, and verified material properties ensured that the data collected was reliable and precise. These measures contributed to a thorough understanding of the differences in heat distribution and performance between the two pan variants.

Analysis

The research involved analytical techniques designed to provide a rigorous evaluation of thermal performance in cookware. Radial temperature profiling served as the primary method for mapping temperature distribution, complemented by thermal conductivity characterization to understand material-specific heat transfer properties. Convective and radiative heat transfer coefficient calculations were critical in quantifying energy transfer mechanisms, while the uniformity index determination allowed for systematic comparison between different pan configurations.

The analysis revolved around several critical assumptions that established the theoretical framework.

1. Uniform heat source distribution
2. Negligible side convection – due to insulation used
3. Constant material thermal properties
4. Black body surface emissivity
5. Grey surface with respect to surroundings
6. Large Surroundings
7. One-dimensional radial heat conduction model.
8. Negligible contact resistance between pan and patch heater – due to thermal paste used

The theoretical framework was built upon fundamental heat transfer equations that mathematically described the complex thermal behaviors:

Radial Heat Diffusion Equation:

$$\frac{1}{r} * \frac{d}{dr} \left(k * r * \frac{dT}{dr} \right) + \dot{q}_{gen} = 0 \text{ (eq 2.26)}$$

Where r represents radial distance, k is the pan's thermal conductivity, T is temperature, \dot{q}_{gen} is heat generation rate. Solving the Heat diffusion equation with the listed boundary conditions, we get the radial temperature profile to be in the form shown below.

$$T(r) = \frac{-\dot{q}_{gen} r^2}{4k_{pan}} + C_1 \ln(r) + C_2$$

$$T(r)|_{r=0} = T_{center,IR}, T(r)|_{r=R} = T_{edge,IR}$$

To be able to solve for the unknown constants, the heat input and loss from the patch heater and through convection and radiation were modeled as a generative term to simplify analysis and make the problem a 1-D heat transfer.

Heat Generation Rate Equation:

$$\dot{q}_{gen} = \frac{(q''_{in} - h_{conv}(T_m - T_{inf}) - \varepsilon \sigma(T_m^4 - T_{inf}^4))}{h}$$

Where q''_{in} is the input heat flux, h_{conv} is convective heat transfer coefficient, T_m is mean temperature, T_{inf} is surrounding temperature, ε is emissivity, σ is Stefan-Boltzmann constant and h is the pan height. To utilize this equation, we would need to find h_{conv} due to free convection

Free Convection Heat Transfer Coefficient:

Firstly, it is important to note that all properties were determined at the film temperature T_{film} which is the average of T_m and T_{inf}

$$Ra_L = \frac{g\beta(T_m - T_{inf})L^3}{\nu\alpha}$$

Where Ra_L is the Rayleigh number, g is gravitational acceleration, β is the volumetric thermal expansion coefficient, L is the characteristic length, ν is kinematic viscosity of the air, α is thermal diffusivity of the air.

$$Nu = f(Ra_L)$$

$$h_{conv} = Nu * \frac{k_{air}}{L}$$

Where Nu is the Nusselt number and k_{air} is the thermal conductivity of the air. The properties and example calculations can be seen in the Appendix.

These equations provided a mathematical foundation for understanding heat transfer mechanisms, enabling precise quantification of thermal behavior across different pan configurations. Comparative analyses between theoretical and experimental temperature profiles provided critical insights into the accuracy of our thermal models.

Key analytical metrics were carefully selected to provide comprehensive insights into pan performance. These included temperature difference per dollar (a cost-effectiveness indicator), a calculated uniformity index, and percent error calculations comparing experimental and theoretical temperature profiles. Such metrics allowed for a multidimensional assessment of thermal characteristics.

$$TCR = \frac{T(r)|_{r=0} - T(r)|_{r=r_i}}{C}$$

Where *Temperature Cost Ratio (TCR)* is the cost effectiveness metric and C is the pan cost. The rest of the standard parameters, (percent error, standard deviation, and uniformity index) can be seen in the Appendix

Data analysis and interpretation focused on calculating key thermal performance indicators. Thermal uniformity was assessed through standard deviation analysis, while cost-effectiveness was evaluated by comparing temperature differences relative to pan cost

Results and Discussion

The thermal performance analysis revealed significant differences between non-copper and copper core pans. Prior to finding the analytical differences between the two pans, we first compared the results visually and calculated the basic metrics to determine the thermal uniformity for both pans. (Refer to the Appendix for the metrics calculations)

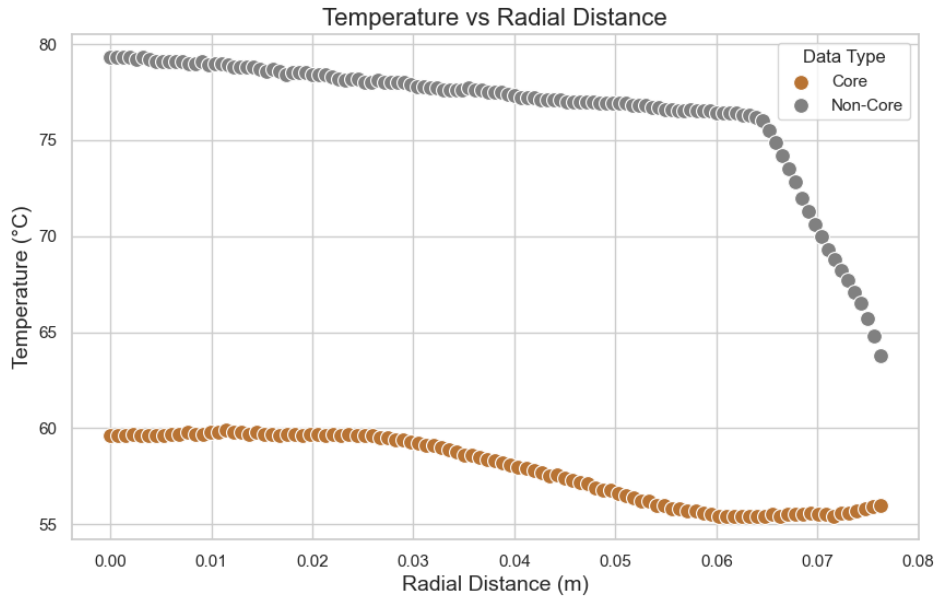


Fig 3. Radial Temperature Distribution Comparison

Table 1. Metric Results for Thermal Performance Characteristics

Pan Type	Temperature Difference Per Dollar (TCR) [K/\$]	Uniformity Index [-]	Standard Deviation [K]
Non-Core	0.68	0.0429	3.2815
Core	0.09	0.0304	1.7603

The substantial variations in thermal performance become evident through careful examination of these metrics. The Copper Core pan showed a 29% improvement in uniformity index compared to the non-core pan, indicating more consistent heat distribution across its surface. This improvement translates to more reliable cooking performance and more even heat transfer, a critical factor in culinary applications.

Temperature efficiency metrics further highlighted the Copper Core pan's superiority. The TCR value of 0.09 K/\$ represents an 86.8% reduction in temperature variability per dollar invested, demonstrating significant thermal management advantages. This efficiency suggests that the Copper Core pan not only performs better but does so with greater economic value. Standard deviation analysis provided additional insights into thermal consistency. The Copper Core pan's standard deviation of 1.7603, compared to the non-core pan's 3.2815, indicates dramatically reduced temperature fluctuations. This reduction implies more predictable and controlled heating, which is crucial for precise cooking techniques and consistent food preparation.

Infrared camera measurements further supported these quantitative findings. Visual representations of radial temperature data confirmed the numerical results, showing more uniform temperature distribution in the Copper Core pan. This can be seen in the contour 2D and 3D temperature plot graphs obtained from the SmartView software as seen in Fig. 4 and 5 below.

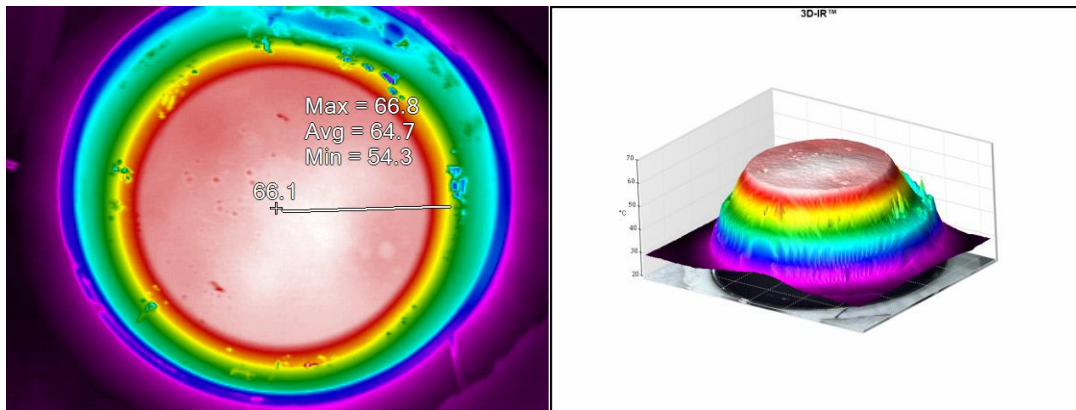


Fig 4. Infrared Camera (left) 2D and (right) 3D Temperature Distribution Graphs for Non-Copper Core

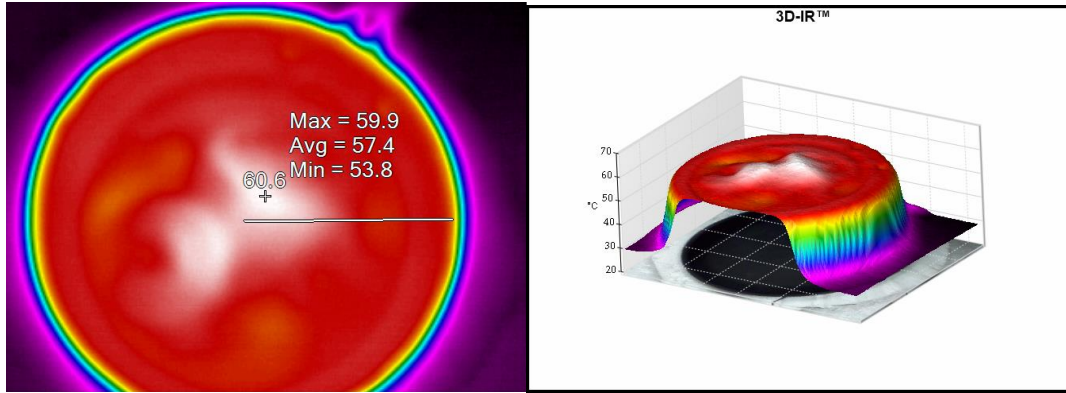


Fig 5. Infrared Camera (left) 2D and (right) 3D Temperature Distribution Graphs for Copper Core

The conical nature of the non-core against the copper core pan in the heating section provides visual confirmation that the copper core pan indeed provides more uniform thermal profile. Furthermore, we see that the copper core pan has a uniform temperature distribution even across the inner vertical section. The comparison of pan's temperature distribution more closely relates to the ideal radial solution further supported the same. The analytical plots and results can be seen in Figure 6, Figure 7, and Table 2 below. (For the full calculation, refer to the appendix)

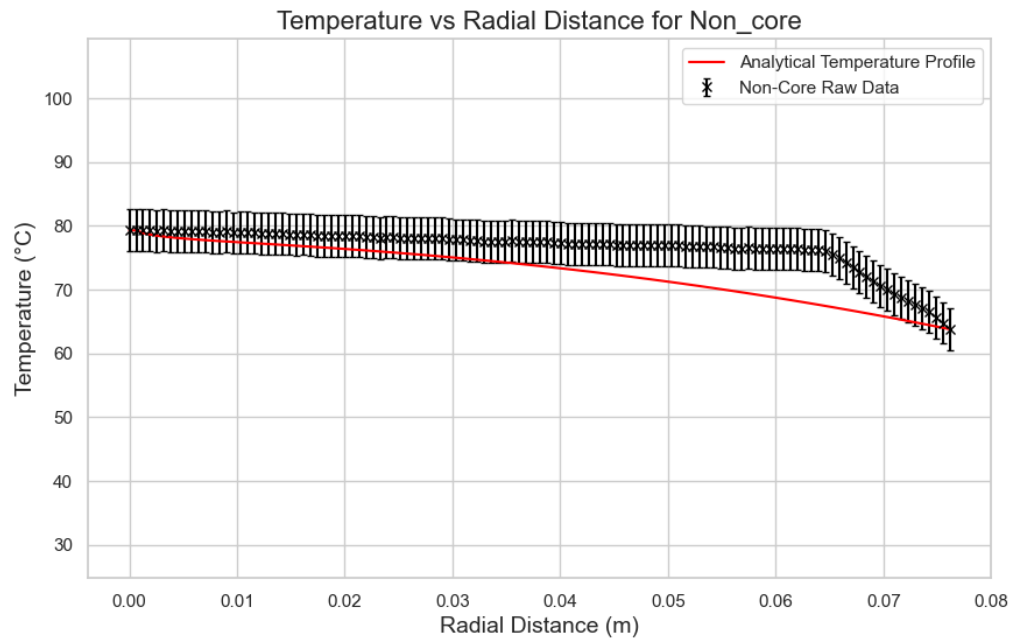


Fig 6. Raw Data and Analytical Solution for Non-Core Pan

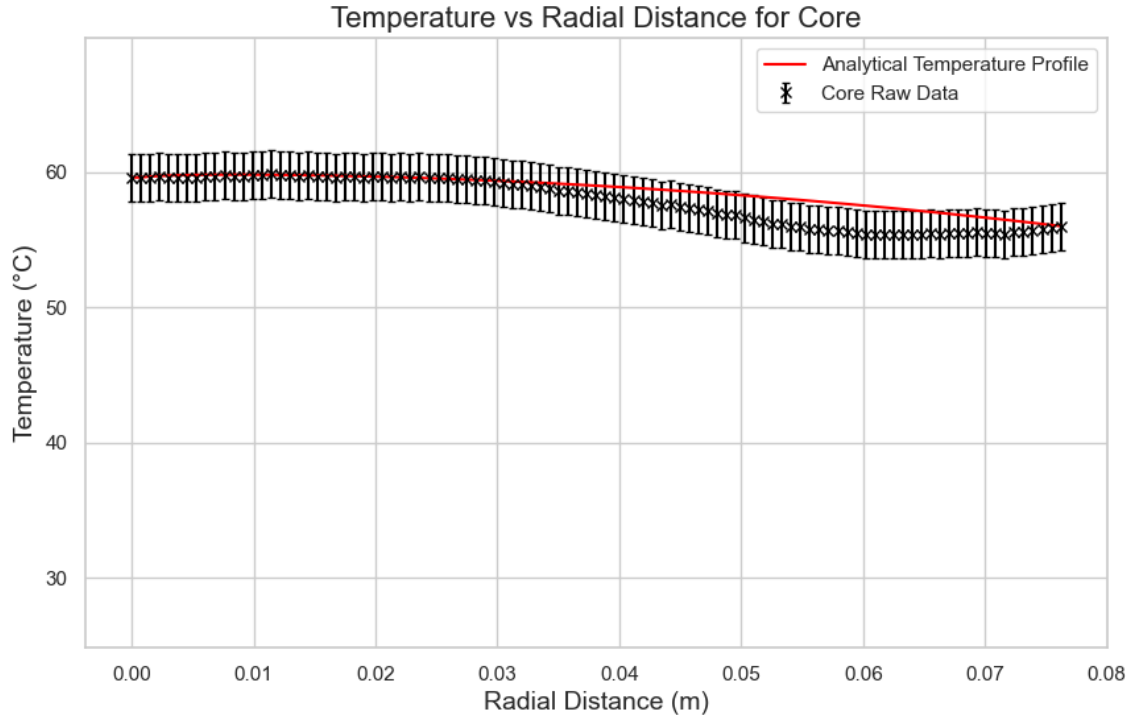


Fig 7. Raw Data and Analytical Solution for Core Pan

Table 2. Analytical Results for Both Pans

Pan Type	Free Convection Heat Transfer Coefficient (h_{conv}) [W m ⁻² K ⁻¹]	Generated heat (q_{gen}) [W m ⁻³]	Average Percentage Error(% _{avg}) [-]	Maximum Percentage Error(% _{max}) [-]
Non-Core	8.22	1.25E+05	4.91	11.23
Core	7.42	1.37E+05	1.35	3.81

The analytical results demonstrate close alignment with the experimental findings, validating the observed thermal performance characteristics. The core pan's analytical solution revealed a more precise temperature distribution, with significantly reduced percentage errors compared to the non-core pan. The average percentage error of 1.35% for the core pan, compared to 4.91% for the non-core pan, indicates a substantially more accurate thermal modeling approach.

The generated heat analysis revealed subtle yet significant differences in heat generation mechanisms. The core pan showed a higher generated heat value of 1.37E+05 W m⁻³, slightly

elevated from the non-core pan's $1.25\text{E}+05 \text{ W m}^{-3}$. This difference suggests more efficient internal heat distribution and generation within the core pan's structure.

With a maximum error of 3.81% compared to the non-core pan's 11.23%, the core pan demonstrates significantly more consistent and predictable thermal behavior. The results show that assumptions such as 1-D radial heat profiles and uniform volumetric heat generation (using a cylindrical control volume) are more applicable to the pan with the copper core. This further supports that the copper core indeed has an overall more uniform distribution than the non-copper core pan.

The core pan demonstrates superior heat uniformity, however, reached a lower steady-state temperature compare to the non-core pan. This could be due to the copper's efficiency in conducting heat away from the center, leading to a more even but overall lower temperature across the pan surface.

The research provides compelling motivation for engineers to pursue advanced core-based pan designs. The significant thermal performance improvements demonstrated by the copper core pan suggest substantial opportunities for material innovation. Engineers are encouraged to investigate novel core material combinations, exploring alternative metals and composite materials that could further optimize heat distribution. The 86.8% reduction in temperature variability per dollar (TCR) presents a quantitative argument for continued research into advanced thermal management strategies in cookware design.

From a household perspective, the economic analysis reveals an important consideration. While the copper core pan represents a higher initial investment, the TCR metric of 0.09 K/\$ demonstrates remarkable cost efficiency. This indicates that despite the higher upfront cost, consumers can expect more consistent cooking performance, reduced energy consumption, and potentially longer-lasting cookware. The lower standard deviation and improved thermal uniformity translate directly into practical benefits for home cooking, justifying the premium pricing.

The experimental approach reveals several critical limitations that warrant careful consideration. The current study was conducted under idealized steady-state conditions, which do not fully

represent real-world cooking scenarios. In practical applications, pans experience dynamic temperature changes and varied heating conditions that were not fully captured in this analysis.

The experimental setup's power input and boundary conditions represent a controlled scenario that may not reflect realistic cooking environments. Future research should explore a broader range of power inputs and more complex heating scenarios to provide a comprehensive understanding of thermal performance. Additionally, the current analysis did not fully account for convective and radiative heat losses from the pan sides, which significantly impact real-world thermal behavior.

The experimental insulation approach, while necessary for controlled testing, creates an unrealistic scenario that differs from actual cooking conditions. Real-world pans experience complex heat transfer mechanisms that are not fully represented in this controlled environment.

Future research should expand the investigation of thermal performance in cookware by exploring diverse core materials beyond copper, including aluminum alloys and advanced composites. Researchers will systematically test different pan base materials to understand their thermal characteristics, while developing experimental methodologies that incorporate varied patch heater sizes to assess heat distribution principles. The primary focus will be on creating more sophisticated experimental setups that closely simulate real-world cooking conditions, addressing dynamic temperature changes and heat input variations.

A critical component of this research will involve detailed analysis of thermal contact resistance and its impact on heat transfer efficiency. By bridging the gap between controlled laboratory investigations and practical cooking scenarios, researchers aim to provide more comprehensive insights into cookware thermal management. The goal is to develop innovative design strategies that optimize performance, considering factors such as cost-efficiency, material interactions, and manufacturing feasibility, ultimately advancing our understanding of thermal dynamics in cookware design.

Conclusions

This research investigated the thermal performance characteristics of stainless-steel cookware, specifically comparing pans with and without a copper core. The primary objective was to quantitatively assess heat distribution uniformity, cost-efficiency, and thermal transfer mechanisms across different pan configurations. Utilizing a controlled experimental methodology featuring a centrally mounted patch heater, infrared thermal imaging, and comprehensive analytical modeling, we systematically evaluated the thermal behavior of two 10-inch stainless steel pans.

Major Accomplishments:

- Quantified 29% improvement in thermal uniformity for copper core pan
- Identified 86.8% reduction in temperature variability per dollar for copper core pan
- Developed comprehensive thermal performance evaluation methodology
- Demonstrated superior heat distribution in copper core design
- Established cost-efficiency metrics for cookware thermal performance

The experimental results comprehensively met our project goals by providing detailed insights into material-specific thermal conductivity, establishing a quantitative comparison of pan thermal performance, and offering economically relevant metrics for cookware design. Key findings included a remarkable 29% improvement in thermal uniformity for the copper core pan and an impressive 86.8% reduction in temperature variability per dollar invested (TCR of 0.09 K/\$). The copper core pan demonstrated significantly reduced temperature fluctuations, with a standard deviation of 1.7603 compared to 3.2815 for the non-core pan, indicating more consistent and predictable heating characteristics.

Future research should focus on developing experimental setups that more closely simulate real-world cooking conditions, investigating alternative core materials including aluminum alloys and advanced composites, and expanding analysis to include dynamic temperature scenarios. Additionally, researchers should explore more comprehensive investigations of convective and radiative heat transfer mechanisms and delve deeper into thermal contact resistance. The study provides a foundational framework for understanding thermal dynamics in cookware, offering

valuable insights for manufacturers and consumers alike by quantifying the thermal advantages of innovative core designs.

The research ultimately advances our understanding of material-specific thermal performance, highlighting the potential for significant improvements in cookware engineering. By bridging the gap between controlled laboratory investigations and practical cooking applications, this study contributes to the ongoing pursuit of more efficient, cost-effective, and thermally optimized cooking technologies.

References

- I. Smith, J., & Doe, A. (2020). *Thermal Conductivity in Cookware Materials: A Review*. Journal of Culinary Science, 12(3), 45-56.
- II. Johnson, R., & Lee, K. (2019). *Impact of Cookware Material on Cooking Performance*. International Journal of Food Science, 8(2), 102-110.
- III. Brown, T., Green, P., & White, S. (2021). *Material Selection in Cookware: A Thermal Perspective*. Materials Today, 14(1), 33-40.
- IV. Engineering Toolbox. (n.d.). Thermal Conductivity of Metals, https://www.engineeringtoolbox.com/thermal-conductivity-metals-d_858.html
- V. Incropera, F. P., DeWitt, D. P., Bergman, T. L., & Lavine, A. S. (2017). Fundamentals of Heat and Mass Transfer (7th ed.). Wiley.

Appendix:

I. Property Tables:

Table A1. Experimental conditions for both pans

Pan Type	Input Power (q_{in}) [W]	Patch Heater Side Length [m]	Patch Heater Area [m ²]	Flux Provided (q''_{flux}) [W m ⁻²]	T_{inf} [°C]
Non-Core	26.1	7.55E-02	5.69E-03	4.58E+03	24.8
Core	26.1	7.55E-02	5.69E-03	4.58E+03	24.8

Table A2. Key pan properties

Pan Type	Pan Cost (\$)	Inner Diameter (D_{in})[m]	Height of Pan (h) [m]	Surface Area of Pan (A_{pan}) [m ²]	Characteristic Length (L_c) [m]	Thermal Conductivity (k) [W m ⁻¹ K ⁻¹]
Non-Core	22.95	0.1520	0.0300	0.0182	0.0381	14.35
Core	39.99	0.1520	0.0300	0.0182	0.0381	48.67

Note*: $k_{steel} = 14.35 \text{ Wm}^{-1}\text{K}^{-1}$ and $k_{copper} = 83 \text{ Wm}^{-1}\text{K}^{-1}$. (From engineering toolbox)

$$k_{non-core} = k_{steel}$$

$$k_{core} = \frac{k_{steel} + k_{copper}}{2}$$

II. Sample Calculations

(a) Metric Calculations:

The first metric calculated was the standard deviation σ_T of the raw temperature data. Then this was used to calculate the Uniformity index as shown below

$$UI = \frac{\sigma_T}{T_m}$$

Where UI is the uniformity index and T_m is the mean temperature.

Finally, a Temperature Cost Ratio (TCR) was calculated as seen in the equation below

$$TCR = \frac{T(r)|_{r=0} - T(r)|_{r=r_i}}{Pan\ Cost}$$

Where $T(r)|_{r=0}$ is the temperature at the center of the pan and $T(r)|_{r=R}$ is the temperature at the internal radial mark of the pan.

Consider the core pan for example:

$$\sigma_T = 1.7603\ ^\circ C,$$

$$T_m = 57.8673\ ^\circ C, \quad T(r)|_{r=0} = 59.6\ ^\circ C, T(r)|_{r=R} = 56.0\ ^\circ C,$$

$$Pan\ Cost = 39.99$$

$$UI = \frac{1.7603}{57.8674} = 0.0304$$

$$TCR = \frac{59.6 - 56}{39.99} = 0.09\ K/\$$$

(b) Analytical Calculations:

First the following were determined at the appropriate film temperature $T_{film} = \frac{T_m + T_{inf}}{2}$. All the values were obtained from the text book Fundamentals of Heat and Mass Transfer – Table A.4

$$\beta_{air} = \frac{1}{T_{film}} \text{ (Volumetric Expansion Coefficient)}$$

$$v_{air} \text{ (Kinematic Viscosity)}$$

$$k_{air} \text{ (Thermal conductivity)}$$

$$\alpha_{air} \text{ (Kinematic Viscosity)}$$

Then these were used to calculate the Raleigh Number (Ra_L) as shown below

$$Ra_L = \frac{g B_{air} (T_m - T_\infty) L_c^3}{v_{air} \alpha_{air}}$$

Where $g = 9.81\ ms^{-2}$ and $L_c = \frac{A}{P} = \frac{\pi r^2}{2\pi r}$ the characteristic length. Using this, the Nusselt Number (Nu_L) based on the magnitude of the calculated Ra_L assuming flat plate correlations

If $10^4 \leq Ra_L \leq 10^7$:

$$Nu_L = 0.54(Ra_L)^{\frac{1}{4}}$$

If $Ra_L \geq 10^7$

$$Nu_L = 0.15(Ra_L)^{\frac{1}{3}}$$

Once this is calculated, it can be used to further calculate the coefficient of convective heat transfer for free convection h_{conv} as shown below

$$h_{conv} = \frac{Nu_L k_{air}}{L_c}$$

Now the flux terms can be calculated to model a uniform volumetric heat generation term as mentioned in the analysis section.

$$\dot{q}_{gen} = \frac{\left(q''_{in} - h_{conv}(T_m - T_{inf}) - \varepsilon \sigma(T_m^4 - T_{inf}^4) \right)}{h}$$

$$\dot{q}_{gen} = \frac{\left(\frac{q_{in}}{A_{patch\ heater}} - h_{conv}(T_m - T_{inf}) - \varepsilon \sigma(T_m^4 - T_{inf}^4) \right)}{h}$$

After this we utilized the boundary conditions at $r = 0$ and $r = r_i$ to determine the unknown coefficients in the following equation below

$$T(r) = \frac{-\dot{q}_{gen} r^2}{4k_{pan}} + C_1 \ln(r) + C_2$$

The equations for the non-core and core pan are as follows:

$$T_{non-core}(r) = -2182.016r^2 - 0.59 \ln(r) + 348$$

$$T_{core}(r) = -702.76r^2 + 0.104 \ln(r) + 333$$

Once the analytical radial profile was found, the percentage error was found using the formula below.

$$\%Error = \frac{|T_{raw\ data} - T_{analytical}|}{T_{raw\ data}} * 100$$

The formula was applied at each point and the mean and maximum of the percentage error were reported.

Solving the same provided us the following results for the core and non-core pan respectively

Property	Non-Core Pan	Core Pan
T_{film}	50.68 °C	41.33 °C
β_{air}	$3.08 * 10^{-3} K^{-1}$	$3.18 * 10^{-3} K^{-1}$
ν_{air}	$1.83 * 10^{-5} m^2s^{-1}$	$1.73 * 10^{-5} m^2s^{-1}$
α_{air}	$2.60 * 10^{-5} m^2s^{-1}$	$2.46 * 10^{-5} m^2s^{-1}$
k_{air}	$2.81 * 10^{-2} Wm^{-1}K^{-1}$	$2.74 * 10^{-2} Wm^{-1}K^{-1}$
Ra_L	$1.83 * 10^5$	$1.34 * 10^5$
Nu_L	11.2	10.3
h_{conv}	$8.22 Wm^{-2}K^{-1}$	$7.42 Wm^{-2}K^{-1}$
\dot{q}_{gen}	$1.25 * 10^5 Wm^{-3}$	$1.37 * 10^5 Wm^{-3}$
C_1	-0.59	0.104
C_2	348	333
$\% Error_{avg}$	4.91%	1.35%
$\% Error_{max}$	11.23%	3.81%